JOURNAL OF NANO- AND ELECTRONIC PHYSICS
Vol. **17** No 2, 02012(6pp) (2025)

ЖУРНАЛ НАНО- ТА ЕЛЕКТРОННОЇ ФІЗИКИ
Том **17** № 2, 02012(6cc) (2025)

OPEN ACCESS

REGULAR ARTICLE

Pulse Duration Effect of Laser Ablation on the Morphology Properties of Gold Nanoparticles Deposited on Porous Silicon

A.A. Sulaiman[1], T.A. Aswad[2], I.B. Karomi[3], S.A. Najim[1,*] ✉

[1] *University of Mosul, College of Science, Department of Physics, 41002 Mosul, Iraq*
[2] *The Directorate General of Education in Salah Al-Deen, Iraq.*
[3] *University of Mosul, College of Education for Pure Science, 41002 Mosul, Iraq*

(Received 28 January 2025; revised manuscript received 18 April 2025; published online 28 April 2025)

Gold nanoparticles recently gaining vast attention owing to their wide range of applications in optical, catalytic, mechanical, and electronic fields. Due to the simplicity approach of generating nanoparticles and free of contamination, laser ablation in liquids is extensive used to yield varied types of nanoparticle structures, including quantum dot, quantum wire, carbon nanotube and core shell nanoparticles. Herein, we report the morphology properties of a gold (Au) nanoparticles prepared by laser ablation in a liquid at different pulse duration (i.e., 300, 30, and 3 ns). The Au nanostructures were then deposited on the PSi layer, prepared by electrochemical etching technique. The samples were characterized by means of SEM, EDS, AFM, and XRD procedures. Results confirmed the formation of the FCC Au nanoparticles structures in nano-scale with pseudo-spherical shapes. The reduction of the pulse width of the ablated laser revealed major effects on the AuNPs, where the average size of them significantly decreases and the homogeneity of the nanoparticles increases as well as an improvement in the samples roughness was recorded. Thus, controlling the pulse width duration can produce specific morphology properties AuNPs for particular applications.

Keywords: Gold nanoparticles, Laser pulse width, Morphology, SEM, EDS, XRD.

DOI: 10.21272/jnep.17(2).02012 PACS numbers: 73.43. – f, 74.25.fc, 78.30. – j

1. INTRODUCTION

Owing to exclusive chemical, optical and electrical properties, gold (Au) nanoparticles have been received massive attention in both preparation and application fields [1-4]. In fact, by controlling the size, shape and the internal structure of the nanoparticle materials, it is possible to manipulate the optical, electrical and mechanical characteristics of these materials, hence, new applications can be emerged [5-8]. This can be achieved in pulsed laser ablation in liquid technique (PLAL) by carful optimized the operation parameter of the laser source, geometric setup of the experiment and the environment of the target [9-14]. Solid state lasers produce low power such as quantum wells and quantum dots semiconductor are usually used for photonic integrated circuits [15-17]. Whereas high power solid state laser such as Nd: YAG and Ti: sapphire lasers, beside the traditional uses in industry, they recently have been widely used in PLAL. This is due to their ability to generated high optical peak power with ultrashort pulse duration in nanosecond and picosecond scales [18, 10, 19]. PLAL technique has been wildly utilized for creating nanostructure materials, due to not only the simplicity of the experimental work, but also the surface free contamination product in comparison with the conventional techniques of growing and fabrication of nanostructures such as thermal oxidation, hydrothermal synthesis, MOVPE, MPE,CBD etc. [20-24]. Therefore, laser ablation in a liquid has recently moved into the spotlight of research for nanoparticles generating. Most of the these researches are focusing on adjusting the size, shape and distribution of the nanoparticles (NPs), by manipulating laser factors and liquid type. For example, the role of a liquid media on the manufacture of MgONPs by nanosecond laser has been reported recently in [25] they found that the smaller particles can be obtained in ethanol and propanol instead of the distilled water. Ablation laser fluence role on the morphology of CuO nanostructure was reported in [26], a red shift in energy bandgap was observed when the ablation period and fluence are increased. Further study involving the influence of ablated laser wavelength influence on gold nanoparticle properties was documented in [27]. It is reported that laser energy can affect the size of the nanoparticle and their distribution [28]. The polarization roles on formation of AgNPs prepared by pulsed laser was documented in [29-31]. Furthermore, it is found that the pulse duration of the ablated laser could strongly affect the sizes of the AlNPs [32]. Nevertheless, there are rarely focused studies on the influence of the pulse width of the ablated laser on the morphological map of gold generated nanoparticles. Here we report the morphology properties of the AuNPs prepared by laser ablation in a liquid at different pulse duration (i.e., 300, 30, and 3 ns). The Au nanostructures have been placed on the PSi prepared by electrochemical etching technique to increase the alignment of the AuNPs.

* Correspondence e-mail: suhaabdullah@uomosul.edu.iq

Cite this article as: A.A. Sulaiman et al., *J. Nano- Electron. Phys.* 17 No 2, 02012 (2025) https://doi.org/10.21272/jnep.17(2).02012

2. EXPERIMENTAL DETAILS

To synthesize gold nanoparticles (AuNPs) from a bulk gold purity of 99.99 %, Q-switched Nd:YAG solid state laser emitting at a second-harmonic generation of 532 nm was utilized to irradiate the bulk gold for 10 min. The gold plate was immersed in a deionized water (15 ml) on a rotated motor for stirring effect as it shown in Figure 1. The laser produces average pulse energy of 20 mJ at a repetition rate of 10 kHz with 4.5 mm spot size and TEM_{00} profile mode. The pulse duration of the laser was varied in this work (300 ns, 30 ns and 3 ns) to study the influence of the pulse width on the generated AuNPs. A 15 cm focal-length convex-lens was used to foci the laser beams on the gold plate.

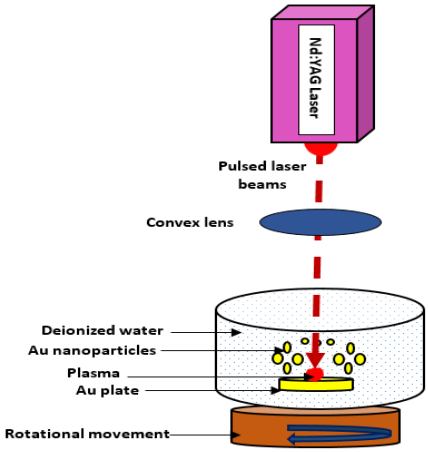

Fig. 1 – Setup of laser ablation in liquid

On the other hand, a *p*-type porous silicon (PSi) were papered in this work using electrochemical etching technique [33-37] as it shows in Figure 2. The prepared porous silicon is used as a substrate for depositing the generated Au nanostructures (AuNPs).

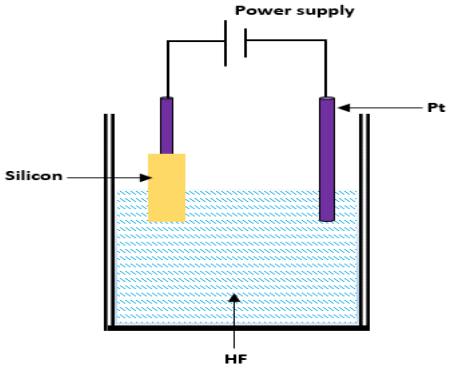

Fig. 2 – Electrochemical etching method

Figure 3a represents the cross-section SEM image for the PSi prepared in this work, the PSi reveals pores structure shape with different sizes (the dimeters of the pores are in the average of 55 nm with estimated maximum lengths of 4.5 μm). These pores are formed due to the dissolution during the electrochemical process. Figure 3b shows the cross-section SEM image for AuNPs generated at 300 ns pulsed duration deposited on the PSi substrate. It can be seen that the Au nanoparticles fill the pore of the PSi substrate.

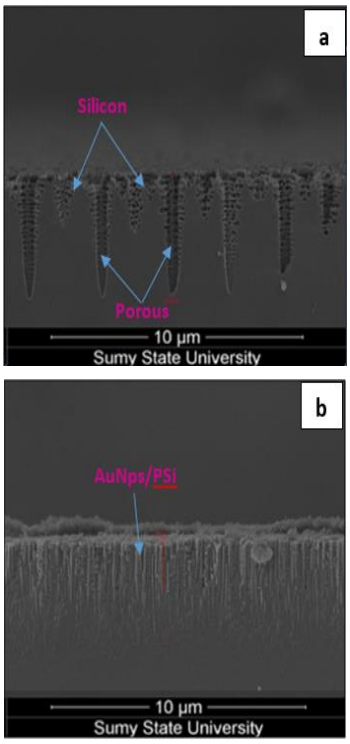

Fig. 3 – Cross-section SEM for porous silicon (a) and for Au nanoparticles prepared at 300 ns on PSi (b)

3. RESULTS AND DISCUSSION

The top-view scan electron microscopy SEM images and the equivalent energy-dispersive X-ray spectroscopy EDS measurements of the Au nanoparticles on PSi prepared by PLAL at different pulse durations (300, 30, and 3 ns) for 10 min of irradiation are presented in Figure 4. The SEM images reveal a pseudo-spherical morphology of the AuNPs of less than 50 nm diameters gathering as cultures due to the pores of the Si-substrate which aligns the metal nanostructures [38-40]. Furthermore, SEM images show a major impact on the shape and the size of the AuNPs when the pulse duration of the ablated laser is reduced. The mean diameter of the AuNPs significantly decreases when the pulse duration in reduced, and density of top-view grain sizes of AuNPs changes with pulse duration. For more understanding the effect of the pulse width of the laser on the size of the formed nanoparticles. It is worth noting the when the pulse hits the target during the ablation process bubbles of a plasma are created, if the pulse time is less than the target thermal diffusion time a quick and small plasma bulb would be created [41]. Therefore, when the pulse width went down from 300 ns to 3 ns, the time of the ablation becomes smaller than the time of the thermal diffusion of the Au, and hence smaller AuNPs are formed in shorted pulse duration. On the other hand, to reveal surface chemical configuration of the samples surface, EDS measurements were conducted as is illustrated in Figure 4. It can be seen that EDS results confirm the presents of the Au on the spectra peak of the samples. The first largest peak in EDS spectra is for Si due to the PSi substrate of the nanoparticles, and oxygen-peaks were recorded in the EDS spectra which are owing to inevitable

contamination, whereas, for C, F, Ca, and Na were presented due to aggregation and formation of gold nanoparticles during preparation process [42]. The chemical configuration recorded from EDS analyses with their atomic weight percentage of the samples at different pulse duration (300, 30, and 3 ns) are labeled in Table 1. The findings indicate that the percentage of the AuNPs element increases with decreasing pulse duration of the lasers. This attributed to the highly aggregated of AuNPs are inside the PSi, where the shortest pulse duration 3 ns creates smaller AuNPs as conformed by the SEM images. Precise work to control the size of self-assembled AuNPs has been reported in [43] through controlling the deposition level and the temperature of annealing. Here, we modified the AuNPs configurations generated by PLAL through only optimizing the pulse duration of the ablated laser.

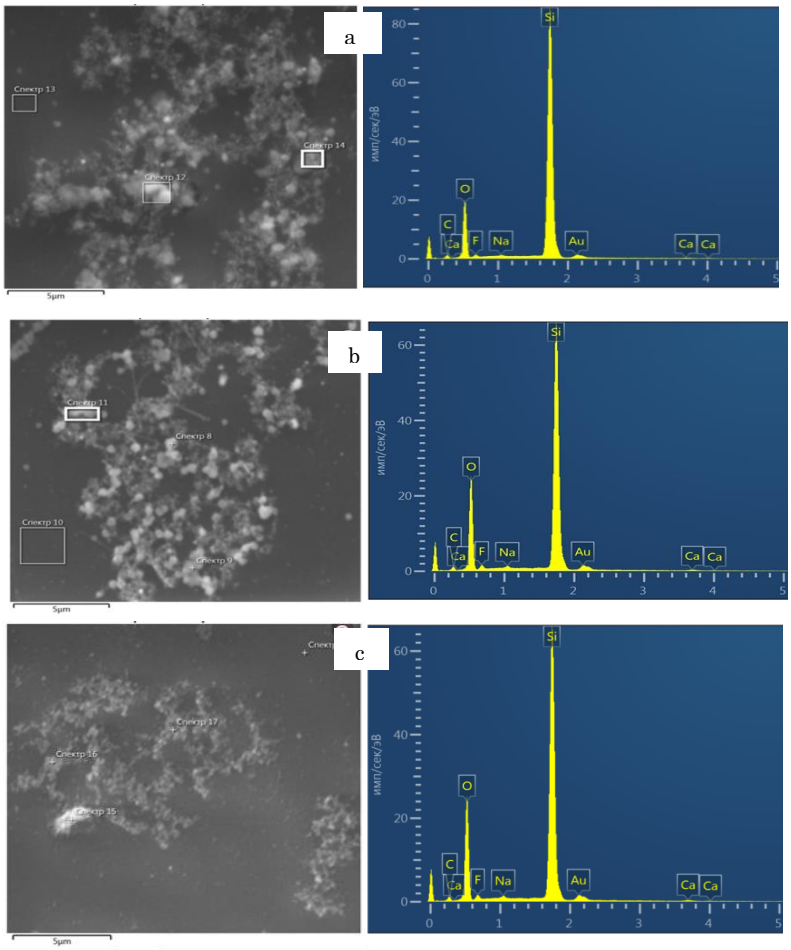

Fig. 4 – SEM with EDX measurements of AuNPs/PSi samples at different pulse durations: (a) 300, (b) 30, and (c) 3 ns

Table 1 – The elemental composition extracted from EDS measurements of the samples at different pulse durations: 300, 30, and 3 ns

Element	Line type	Atom % 300 ns	Atom % 30 ns	Atom % 3 ns
O	K-Series	21.59	28.40	19.89
F	K-Series	0.92	1.47	1.52
Si	K-Series	68.14	59.11	57.53
C	M-Series	4.40	3.99	6.57
Au	K-Series	4.41	6.00	13.01
Na	K-Series	0.20	0.37	0.45
Ca	K-Series	0.34	0.66	1.04
Total %		100	100	100

Microscopic imaging of Au nanoparticles on PSi samples was implemented using atomic force microscopy AFM tool. Figure 5 shows the Au nanoparticles on PSi prepared by PLAL at different pulse durations (300, 30 and 3 ns) for 10 min of irradiation. The AFM images confirm the presents of Au nanoparticles with the average dimeters around 30 nm. The pulse duration shows a substantial effect on the size and the roughness of the samples. The AFM images are in agreement with the SEM images, where both showed a reduction of the Au nanoparticles sizes with reducing laser pulse duration. Moreover, the AFM results show that the distribution of Au nanoparticles on a PSi wafer becomes more homogenous when the pulse duration of the laser gets shorter. Furthermore, Figure 5c reveals the mappings of the elements silicon, gold, carbon, and oxygen, respectively, which are in agreement with the EDX measurements presented in Figure 4. Additionally, the size of the Au nanoparticles was in agreement with SEM, and it is more possible to notice the shape of the structures clearly usually the AFM images reveal the shape of the nanoparticles more clearly than the TEM ones [44]. The root mean square roughness (R_{rms}) of the

samples was estimated from the AFM images by means of J program and found to be 3.874, 3.7893, and 3.343 nm for the pulse duration, 300, 30, and 3 ns respectively. It can be seen that the roughness of the sample is improved when the pulse duration is reduced. Those results show that the characterizations of the Au nanoparticles can be significantly developed by controlling the pulse duration of the lasers during the ablation process of the gold target.

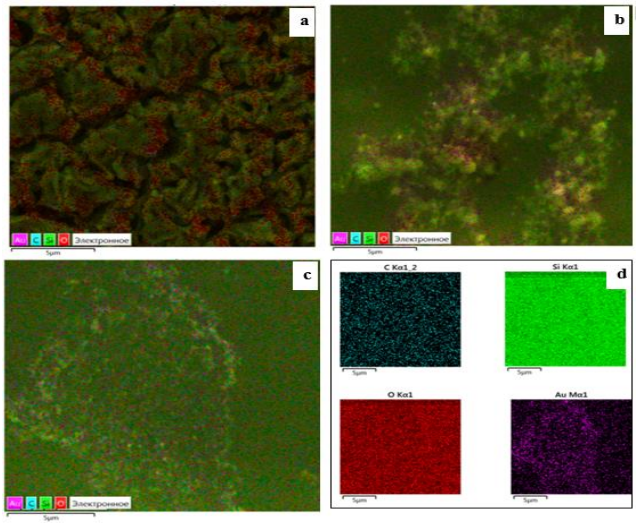

Fig. 5 – AFM measurements of AuNPs/PSi samples at different pulse durations: (a) 300, (b) 30, and (c) 3 ns and (d) is the mappings of the elements

In order to study the crystallinity of synthesized Au nanoparticles on PSi samples, X-ray diffraction XRD measurement was utilized. The corresponding XRD patterns of the AuNPs on PSi prepared by PLAL at different pulse durations (300, 30, and 3 ns) for 10 min of irradiation are shown in Figure 6. The gold nanoparticles exhibited two distinctive peaks, the first one at $2\theta \approx 31.5$ and 50.2 match the Bragg reflections (100) and (220) of face center cubic (FCC) lattice, respectively. Figure 6 shows that the XRD patterns affect by laser pulse duration and the patterns showed more crystallized for the AuNPs samples prepared at 3 ns pulse duration. Moreover, the peak of Si wafer appears more clearly at 3 nm pulse duration at $2\theta \approx 65.3$ matching (100) Bragg reflection orientation. To estimate the Au average grain size of the AuNPs/PSi at different pulse durations, Debye-Scherer equation [45] was used, which is given as:

$$D = \frac{k\lambda}{B\cos\theta} \quad (1)$$

Here, D represents the typical size of AuNPs, K is the Debye Scherer's coefficient (0.94), λ is the photon wavelength of the X-ray source (0.154 nm), B is the FWHM of peak and θ is the Bragg angle of the peak in XRD pattern. The Au average grain size of the AuNPs/PSi at different pulse duration derived from the XRD patterns data are labeled in Table 2.

The result in Table 2 shows that the estimated size of the AuNPs for both observed peaks, (100) and (220) reduces when the pulse duration of Nd:YAG is reduced.

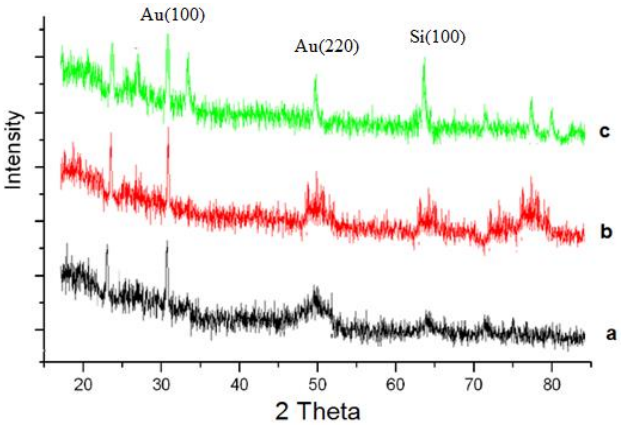

Fig. 6 – XRD patterns of AuNPs/PSi samples at different pulse durations: (a) 300, (b) 30 and (c) 3 ns

Table 2 – Average size of the AuNPs measured Debye-Scherer equation

Pulse Duration (ns)	AuNPs Orientation	Size D (nm)
300	(100)	22.8
	(220)	19.14
30	(100)	19.08
	(220)	17.14
3	(100)	14.6
	(220)	11.76

The results of XRD are reliable with the results of SEM and AFM, where the shorter pulse duration decreases the size of the AuNPs and increases the homogeneity of the structures. Recent work reported the effect of reducing pulse width of the laser on the structure of the generated aluminum nanoparticles showed to be essential for morphological properties of the nanostructures [28]. Furthermore, a significant decrease in the average diameter of AgNPs when the pulse width of the ablated laser is reduced was presented in [43]. These results agree with our results in this work for AuNPs.

CONCLUSIONS

Gold nanoparticles were manufactured by laser ablation technique in deionized water at different pulse widths laser 300, 30 and 3 ns. The AuNPs were deposited on porous silicon wafer prepared by electrochemical etching method. The AuNPs/PSi were tested to reveal their morphological properties by SEM, EDX, AFM and XRD spectroscopy. Reducing of the pulse duration of the ablated laser showed major effect on the properties of the Au prepared nanostructures. SEM and EDX results confirm the presents of the AuNPs with a pseudo-spherical shape of the of less than 50 nm size and their size reduced with reducing pulse width. AFM images exhibited a decrease in the Au nanoparticles size and an improvement in the samples roughness when pulse width is reduced. X-ray diffraction XRD patterns revealed FCC structure of the Au nanoparticles. Additionally, by applying Scherer method to XRD profile Au nanoparticle average sizes were estimated at different pulse duration. The shortest pulse duration could reduce the plasma bubbles size during the ablation

process when the pulse width becomes shorter than gold thermal diffusion time, so the size of the gold nanoparticles is reduced. These results indicated the possibility of precisely controlling the AuNPs morphological properties by modifying the pulse duration of the laser during the ablation process. This could open the possibility of generating AuNPs with specific morphological properties for particular required applications.

REFERENCES

1. S.R Devi, A.G. Siddharth, *Appl. Biochem. Biotechnol.* **194**, 4187 (2022).
2. L. Ge, Q. Li Wang, M. Ouyang, J. Li X., M.M. Xing, *Int. J. Nanomedicine* **9**, 2399 (2014).
3. M.S. Muthu, B. Wilson, *Nanomedicine* **5** No 2, 169 (2010).
4. V. Haribabu, K. Girigoswami, A. Girigoswami, *Nano-Struct. Nano-Objects* **25**, 100636 (2021).
5. P. Slepicka, N.S. Kasalkova, J. Siegel, Z. Kolska, V. Švorcik *Materials (Basel)* **18**, No 13(1), 1 (2019).
6. P. Ghosh, G. Han, M. De, C.K. Kim, V.M. Rotello, *Adv. Drug Deliv. Rev.* **60**, 1307 (2008).
7. P.V. Kamat, *J. Phys. Chem. B* **106**, 7729 (2002).
8. G.P. Sahoo, S. Basu, S. Samanta, A. Misra, *J. Exp. Nanosci.* **10**, 690 (2014).
9. L. Korosi, *J. Chem.* **2016**, 4143560 (2016).
10. W. Norsyuhada, W.M. Shukri, N. Bidin, S. Islam, G. Krishnan, *J. Nanosci. Nanotechnol.* **18** No 7, 4841 (2018).
11. G.G. Ali, M.A. Ahmed, A.A Sulaiman, *Digest J. Nanomater. Biostruct.* **17** No 2, 473 (2022).
12. M.M. Al-Maher, N. I. Al-Barhawi, M.A. Al-Jubbori, *J. Educat. Sci.* **30** No 2, 128 (2021).
13. S. Moniri, M.R. Hantehzadeh, M. Ghoranneviss, *Opt. Quant. Electron.* **49**, 174 (2017).
14. N.M.A. Fadhi, F.M. Jasim, *J. Educat. Sci.* **30** No 4, 69 (2021).
15. R.J. Hussin, I.B. Karomi, *Res. Opt.* **12**, 100452 (2023).
16. M.S. Al-Ghamdi, N.M. Almalky, R. Sait, S. Gillgrass, I.B. Karomi, *Opt. Mater.* **145**, 114475 (2023).
17. R.J. Hussin, I.B. Karomi, *AIP Conf. Proc.* **3036** No 1, 050016 (2024).
18. J.C.E. Coyle, A.J. Kemp, J.M. Hopkins, A.A. Lagatsky, *Opt. Express* **26**, 6826 (2018).
19. M.J. Damzen, R.P.M. Green, G.J. Crofts, *Opt. Lett.* **17**, 1331 (1992).
20. J.M.J. Santillan, F.A. Videla, M.B.F. van Raap, D.C. Schinca, L.B. Scaffardi, *J. Appl. Phys.* **113**, 134305 (2013).
21. A.G.S Al-Azzawi, A. Iraqi, Sh.B. Aziz, Y. Zhang, A.R. Murad, J.M. Hadi, D.G. Lidzey, *International Journal of Electrochemical Science* **16** No 12, 21125 (2021).
22. N.G. Semaltianos, S. Logothetidis, N. Frangis, I. Tsiaoussis, W. Perrie, G. Dearden, *Chem. Phys. Lett.* **496**, 113 (2010).
23. A.H. Attallah, F.S. Abdulwahid, Y.A. Ali, *Plasmonics* **18**, 1307 (2023).
24. S.A. Najim, *J. Nano- Electron. Phys.* **16** No 3, 03032 (2024).
25. H. Pereira, C.G. Moura, G. Miranda, F.S. Silva, *Opt. Laser Technol.* **142**, 107181 (2021).
26. H.D. Aghdam, H. Azadi, M. Esmaeilzadeh, S.M. Bellah, R. Malekfar, *Opt. Mater.* **91**, 433 (2019).
27. E. Giorgetti, M.M. Miranda, P. Marsili, D. Scarpellini, F. Giammanco, *J. Nanopart. Res.* **14**, 648 (2012).
28. P. Maneeratanasarn, T.V. Khai, B.G. Choi, K.B. Shim, *J. Korean Cryst. Growth Cryst. Technol.* **22** No 3, 134 (2012).
29. M. Kaempfe, G. Seifert, K.J. Berg, *Eur. Phys. J. D* **16**, 237 (2001).
30. M.I. Ismael, G.G. Ali, *J. Educat. Sci.* **30** No 4, 28 (2021).
31. M.T.I. Allhiby, M.S.H. Al Juboori, *J. Educat. Sci.* **31** No 4, 10 (2022).
32. K.Z. Hang, D.S. Ivanov, R.A. Ganeev, G.S. Boltaev, P.S. Krishnendu, S.C. Singh, M.E. Garcia, I.N. Zavestovskaya, C. Guo, *Nanomaterials* **9**, 767 (2019).
33. D.T. Cao, C.T. Anh, L.T.Q. Ngan, *Advanced Science, Engineering and Medicine* **11** No 12, 1218 (2019).
34. G.G Ali, I.B. Karomi, A.A. Sulaiman, A.M. Mohammed, *Nucl. Instrum. Meth. Phys. Res. Sect. B* **468**, 23 (2020).
35. G. Gh. Ali, A.A. Sulaiman, I.B. Karomi, *AIP Conf. Proc.* **2034**, 020009 (2018).
36. A.A. Sulaiman, *Raf. J. Sci.* **27** No 3, 173 (2018).
37. A.A. Sulaiman, A.A.K. Muhammed, M.M. Ivashchenko, *J. Nano- Electron. Phys.* **11** No 5, 05025 (2019).
38. T.S.T. Amran, M.R. Hashim, N.K.A. Al-Obaidi, *Nanoscale Res. Lett.* **8**, 35 (2013).
39. S.A. Najim, K.M. Muhammed, A.D. Pogrebnjak, *J. Nano-Electron. Phys.* **13** No 4, 04028 (2021).
40. S.A. Najim, N.Y. Jamil, K.M. Muhammed, *J. Nano- Electron. Phys.* **11** No 2, 02003 (2019).
41. A. Subhan, A.I. Mourad, Y. Al-Douri, *Nanomaterials* **22**, 12(13), 2144 (2022).
42. M.Y. Li, M. Sui, P. Pandey, et al., *Cryst. Eng. Comm.* **18**, 3347 (2016).
43. A.E.F. Oliveira, A.C. Pereira, M.A.C. Resende, L.F. Ferreira, *Analytica* **4**, 250 (2023).
44. J.I. Langford, A.J.C. Wilson, *J. Appl. Cryst.* **11**, 102 (1978).
45. J.W. Jeon, S. Yoon, H.W. Choi, J. Kim, D. Farson, S.H. Cho, *Appl. Sci.* **8**, 112 (2018).

Вплив тривалості імпульсу лазерної абляції на морфологічні властивості наночастинок золота, нанесених на пористий кремній

A.A. Sulaiman[1], T.A. Aswad[2], I.B. Karomi[3], S.A. Najim[1]

[1] *University of Mosul, College of Science, Department of Physics, 41002 Mosul, Iraq*
[2] *The Directorate General of Education in Salah Al-Deen, Iraq.*
[3] *University of Mosul, College of Education for Pure Science, 41002 Mosul, Iraq*

Наночастинки золота останнім часом привертають велику увагу завдяки широкому спектру застосування в оптичній, каталітичній, механічній та електронній галузях. Завдяки простоті підходу до створення наночастинок та відсутності забруднення, лазерна абляція в рідинах широко використовується для отримання різноманітних типів структур наночастинок, включаючи квантові точки, квантові дроти, вуглецеві нанотрубки та наночастинки з серцевиною-оболонкою. У цій статті ми повідомляємо

про морфологічні властивості наночастинок золота (Au), отриманих лазерною абляцією в рідині з різною тривалістю імпульсу (тобто 300, 30 та 3 нс). Потім наноструктури Au були нанесені на шар PSi, отриманий методом електрохімічного травлення. Зразки були охарактеризовані за допомогою SEM, EDS, AFM та XRD. Результати підтвердили формування структур наночастинок Au з ГЦК у наномасштабі з псевдосферичними формами. Зменшення тривалості імпульсу абляційного лазера виявило значний вплив на AuNPs, де їх середній розмір значно зменшується, а однорідність наночастинок збільшується, а також було зафіксовано покращення шорсткості зразків. Таким чином, контроль тривалості імпульсу може забезпечити специфічні морфологічні властивості AuNPs для практичних застосувань.

Ключові слова: Наночастинки золота, Ширина лазерного імпульсу, Морфологія, SEM, EDS, XRD.